

Modelling contagious viral dynamics: a kinetic approach based on mutual utility

Giulia Bertaglia* Lorenzo Pareschi^{†‡} Giuseppe Toscani^{§¶}

January 2, 2024

Abstract. The time evolution of a contagious viral disease is modeled as the dynamic progression of different classes of populations that interact pairwise, aiming to improve their condition with respect to a given target. This evolutionary mechanism is based on binary interactions between agents, designed to enhance their utility mutually. To achieve this goal, we introduce kinetic equations of Boltzmann type to describe the time evolution of the probability distributions of the agent system undergoing binary interactions. The fundamental idea is to describe these interactions using principles from price theory, particularly by employing Cobb-Douglas utility functions for the binary exchange and the Edgeworth box to depict the common exchange area where utility increases for both agents.

Keywords. Kinetic models, Epidemic models, Cobb-Douglas utility function, Edgeworth box, Boltzmann-type equations

Contents

1	Introduction	2
2	The model	3
2.1	A Boltzmann-type dynamics	3
2.2	Characterization as compartmental models	4
3	Virus-agent interaction based on mutual utility	7
3.1	Edgeworth box and Cobb-Douglas utility function	8
3.2	A viral interaction model	9
4	Numerical tests	14
5	Conclusion	21

*Department of Environmental and Prevention Sciences, University of Ferrara, Italy.

e-mail: giulia.bertaglia@unife.it

[†]Maxwell Institute and Department of Mathematics, Heriot-Watt University, Edinburgh, UK.

e-mail: l.pareschi@hw.ac.uk

[‡]Department of Mathematics and Computer Science, University of Ferrara, Italy.

e-mail: lorenzo.pareschi@unife.it

[§]Department of Mathematics, University of Pavia, Italy.

e-mail: giuseppe.toscani@unipv.it

[¶]IMATI, Institute for Applied Mathematics and Information Technologies “Enrico Magenes”, Pavia, Italy

1 Introduction

Complex processes in biological systems at microscopic and macroscopic scales can be fruitfully described by means of methods of kinetic theory [2], and, as recently discussed in [3], in many cases the concept of entropy plays an important role. In addition to examples related to irreversible chemical reactions [30], where irreversibility can be described in terms of the monotonicity of entropy, other concepts, like measures of information, are frequently discussed in relation to living systems and the influence on fluctuations (cf. [14] and the references therein).

In this paper, we approach irreversibility in biological processes by means of the concept of utility, and the main example we present is related to viral evolution [13,23]. This approach is complementary to others [10,11], where game theory is used to model the viral behavior, and takes its cue from a well-known model of microeconomics: the Edgeworth box [29].

Although the modeling introduced lends itself to describing various biological phenomena with irreversible nature, in this manuscript, as a prototypical context, we will focus on viral evolution motivated by the recent interest in the dynamics of infectious diseases after the Covid-19 epidemic [4,6–8,20]. Although the evolution of Covid-19, as in the case of other diseases with seasonal characteristics [22,24], has not had a monotonic behavior in moving from a high-risk pandemic phenomenon to a low-risk endemic phenomenon, but rather a behavior similar to that of damped oscillations (successive pandemic waves with decreasing impact), the irreversibility of the phenomenon remains evident.

In the sequel, we will study the evolution of the pandemic by hypothesizing that in the agent-virus interaction it is convenient for both to improve utility, understood for the individual as an optimal balance between sociality and the risk of contracting the disease, and for the virus an optimal balance between contagiousness and adverse effects on the guest.

To this aim, we will introduce kinetic equations of Boltzmann type designed to describe the evolution in time of the probability distributions of the system agent-virus undergoing binary *interactions*. The leading idea is to describe the interactions by means of some fundamental rules in price theory, in particular by using Cobb-Douglas utility functions for the binary exchange, and the Edgeworth box for the description of the common exchange area in which utility is increasing for both agents. We refer to [1] for an introduction to kinetic models in epidemic dynamics.

To verify the irreversibility of the disease in consequence of the undergoing interactions, we refer to the simple classical SIR model of compartmental epidemiology, a statistical model that goes back to the pioneering work of Kermack and McKendrick [21]. Nevertheless, at the price of an increasing difficulty in simulations, the proposed approach can easily be extended to more complex compartmentalization, which is better suited to the study of specific real epidemic phenomena [5,9,18,19]. Numerical experiments will help to clarify the importance of the mechanism in driving the phenomenon towards endemicity.

The rest of the manuscript is organized as follows. In Section 2 we describe the general structure of the mathematical model under consideration and illustrate its relationships with classical compartmental models. Then, Section 3 is devoted to present the competitive mechanism at the basis of the viral evolution inspired by the Edgeworth box theory in economics. We illustrate the behavior of the models with the aid of some numerical experiments in Section 4. Some concluding remarks end the manuscript.

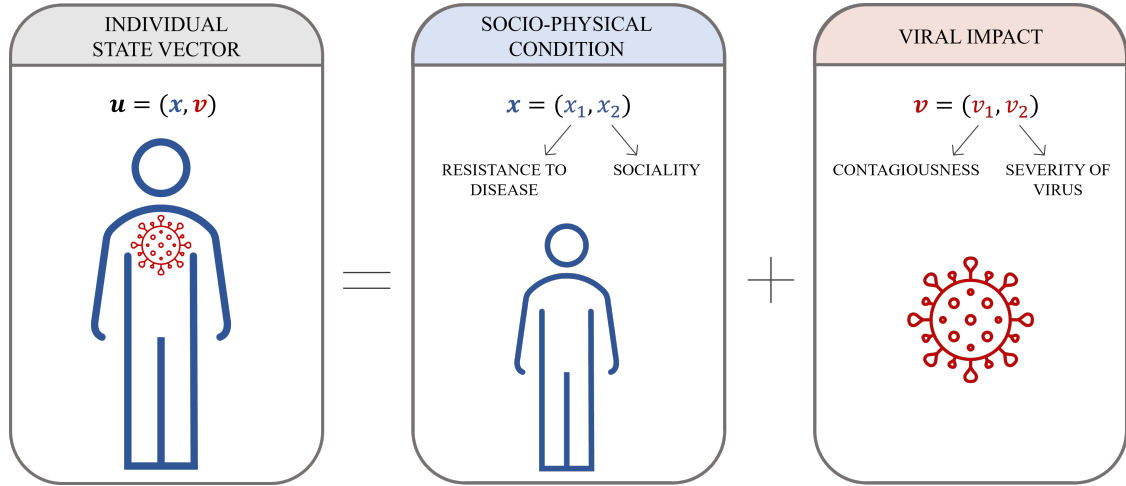


Figure 2.1: Schematic summary of the components of the individual state vector. The individual state is identified by a joint state vector $\mathbf{u} = (\mathbf{x}, \mathbf{v})$, where the *socio-physical condition* vector $\mathbf{x} = (x_1, x_2)$, dependent on the personal rate of resistance to the disease (x_1) and the degree of sociality (x_2), refers to the individual, while the *viral impact* vector $\mathbf{v} = (v_1, v_2)$, composed by the degree of contagiousness (v_1) and the severity of the disease (v_2), refers to the virus.

2 The model

2.1 A Boltzmann-type dynamics

Given a population of individuals, we denote by $f(\mathbf{u}, t)$, with $\mathbf{u} = (u_1, u_2, \dots, u_n)$, $n \geq 2$, the statistical distribution of individuals which are characterized by a state vector $\mathbf{u} \in \mathbb{R}^n$ at time $t \geq 0$.

Having in mind to study the evolution of a pandemic, and believing it important to be able to characterize its evolution in terms of both its infectiousness and its severity, we identify the state vector as the joint state vector $\mathbf{u} = (\mathbf{x}, \mathbf{v})$, where the two-states vectors $\mathbf{x} = (x_1, x_2)$ and $\mathbf{v} = (v_1, v_2)$ refer to the individual and, respectively, to the virus.

In detail, we characterize the state of individuals in terms of their mental and physical well-being. To this aim, we indicate with $x_1 \geq 0$ the personal rate of resistance to disease, which generally depends on both physical state and age, and with $x_2 \geq 0$ the individual's degree of sociality, which can be measured by the mean number of social contacts during a fixed period of time. We will give this state \mathbf{x} the name of *socio-physical condition*.

Likewise, following [25], we characterize the state of the virus in terms of its main features, represented by the degree of infectiousness, measured by $v_1 \geq 0$, and the degree of severity of the disease, measured by $v_2 \geq 0$. We will give this state \mathbf{v} the name of *viral impact*. Clearly, individuals that have not been infected will be characterized by a viral impact $\mathbf{v} = \mathbf{0}$. A schematic summary of the components of the state vector is presented in Figure 2.1. In what follows we will assume that all the state variables can vary between 0 and 1.

The evolution of the densities f , due to the interaction of two agents characterized by the initial state (\mathbf{x}, \mathbf{v}) and (\mathbf{y}, \mathbf{w}) , can be described by a homogeneous Boltzmann-type dynamics [12, 27, 28]:

$$\frac{\partial f(\mathbf{x}, \mathbf{v}, t)}{\partial t} = Q(f, f)(\mathbf{x}, \mathbf{v}, t), \quad (2.1)$$

where $Q(f, f)$ is the bilinear interaction/collisional operator, defined as

$$Q(f, f)(\mathbf{x}, \mathbf{v}, t) = \int_{\mathbb{R}_+^4} \kappa(\mathbf{x}, \mathbf{y}, \mathbf{v}, \mathbf{w}) [f(\mathbf{x}^*, \mathbf{v}^*, t)f(\mathbf{y}^*, \mathbf{w}^*, t) - f(\mathbf{x}, \mathbf{v}, t)f(\mathbf{y}, \mathbf{w}, t)] d\mathbf{y}d\mathbf{w}. \quad (2.2)$$

Here, the star state vectors $(\mathbf{x}^*, \mathbf{v}^*)$ and $(\mathbf{y}^*, \mathbf{w}^*)$ are the post-interaction states of the two agents, and κ is an appropriate function defining the kernel of the interaction, which may depend, in general, by all the state variables of the agents.

As typical in kinetic theory [27], the interaction operator can be seen as the difference between a gain and a loss term of the evolutionary dynamics, $Q(f, f) = Q^+(f, f) - Q^-(f, f)$. In this case, the two operators read

$$\begin{aligned} Q^+(f, f)(\mathbf{x}, \mathbf{v}, t) &= f(\mathbf{x}^*, \mathbf{v}^*, t) \int_{\mathbb{R}_+^4} \kappa(\mathbf{x}, \mathbf{y}, \mathbf{v}, \mathbf{w}) f(\mathbf{y}^*, \mathbf{w}^*, t) d\mathbf{y}d\mathbf{w} \\ Q^-(f, f)(\mathbf{x}, \mathbf{v}, t) &= f(\mathbf{x}, \mathbf{v}, t) \int_{\mathbb{R}_+^4} \kappa(\mathbf{x}, \mathbf{y}, \mathbf{v}, \mathbf{w}) f(\mathbf{y}, \mathbf{w}, t) d\mathbf{y}d\mathbf{w}. \end{aligned} \quad (2.3)$$

Let us conclude this brief introduction to the model noticing that, in the considered infectious dynamics, the operator (2.2) is nonzero only when an infected and a not yet infected individual (susceptible to infection) are interacting with each other. In all the other cases, the interaction dynamics does not produce any effective update of the state of the agents.

2.2 Characterization as compartmental models

We now characterize the modeling just described by considering a classical SIR partitioning of the population, which allows us to highlight how the proposed model, in fact, can easily trace the classical compartmental approach widely used in the epidemiological mathematics literature.

In the SIR compartmental model, the initial population is divided into susceptible (S), who can contract the disease, infected (I), who have already contracted it and can transmit it, and removed (R), who either recovered from the disease and became immune to it or deceased. In terms of state variables of the kinetic approach introduced in the previous section, for a given time $t \geq 0$, we will assume that the distribution f_S of the population of susceptible (not infected) individuals depends only on their socio-physical conditions, as given by the state vector $(\mathbf{x}, \mathbf{0})$. To maintain memory that distributions are generally dependent on the full vector \mathbf{u} , we will write $f_S = f_S(\mathbf{x}, \mathbf{v}, t) = F_S(\mathbf{x}, t) \cdot \delta(\mathbf{v} = \mathbf{0})$, where $\delta(\mathbf{v} = \mathbf{0})$ denotes the Dirac delta function located in the point $\mathbf{v} = \mathbf{0}$. Unlike the class of susceptible, the distribution f_I of the population of infected individuals depends on the full vector state, $f_I = f_I(\mathbf{x}, \mathbf{v}, t)$. Last, to maintain memory of the fact that recovered individuals were infected with the virus, their distribution f_R will be assumed to depend of the vector state $(\mathbf{x}, \mathbf{v}_0)$, where $\mathbf{v}_0 = (0, v_2)$, and it will be denoted by $f_R = f_R(\mathbf{x}, \mathbf{v}, t) = F_R(\mathbf{x}, t) \cdot \delta(\mathbf{v} = \mathbf{v}_0)$. In other words, recovered individuals are characterized by an infectiousness equal to zero. Here, it is important to remark that the value of v_2 could fruitfully be used to measure the percentage of infectious people that do not survive to the disease. This can be obtained by imposing an upper bound \hat{v}_2 above which the infectious individual do not move to the compartment of recovered people. Hence recovered individuals are characterized by a value $\mathbf{v}_0 = (0, v_2)$, in which $v_2 < \hat{v}_2$.

The knowledge of the functions $f_J(\mathbf{u}, t)$, $J \in \{S, I, R\}$ allows to compute all relevant observable quantities. In particular, the distributions at time $t \geq 0$ of the socio-physical states of the sub-populations of susceptible, infected and recovered people are given by the

integrals

$$F_J(\mathbf{x}, t) = \int_{\mathbb{R}_+^2} f_J(\mathbf{x}, \mathbf{v}, t) d\mathbf{v}, \quad (2.4)$$

Hence, the integrals

$$J(t) = \int_{\mathbb{R}_+^2} F_J(\mathbf{x}, t) d\mathbf{x}, \quad J \in \{S, I, R\} \quad (2.5)$$

denote the fractions at time $t \geq 0$ of the three sub-populations. Analogously one can compute moments, defined, for any given constant $\gamma > 0$ by

$$m_{J,i}^\gamma(t) = \frac{1}{J(t)} \int_{\mathbb{R}_+^2} x_i^\gamma F_J(\mathbf{x}, t) d\mathbf{x}, \quad J \in \{S, I, R\}, i = 1, 2.$$

The mean values, corresponding to $\gamma = 1$, are denoted by $m_{J,i}(t)$, $J \in \{S, I, R\}$, $i = 1, 2$. Clearly, choice $i = 1$ corresponds to assessing, at time $t \geq 0$, the average disease resistance of the classes, while choice $i = 2$ gives the average sociality of the classes.

On the pandemic side, the distribution of the virus in the infected class coincides with the integral

$$P(\mathbf{v}, t) = \int_{\mathbb{R}_+^2} f_I(\mathbf{x}, \mathbf{v}, t) d\mathbf{x}, \quad (2.6)$$

and its intensity equals the integral

$$p(t) = \int_{\mathbb{R}_+^2} P(\mathbf{v}, t) d\mathbf{v}. \quad (2.7)$$

As before, one can compute moments through the formula

$$m_i^\gamma(t) = \frac{1}{p(t)} \int_{\mathbb{R}_+^2} v_i^\gamma P(\mathbf{v}, t) d\mathbf{v}, \quad i = 1, 2. \quad (2.8)$$

The mean values $m_i(t)$, corresponding to $\gamma = 1$, give the average infectiousness of the virus at time $t \geq 0$ ($i = 1$), and, respectively its average severity at time $t \geq 0$ ($i = 2$).

Leaving aside for the moment the healing dynamic (hence the R compartment), the evolution of the densities f_J , $J \in \{S, I\}$, replicates the Boltzmann equation (2.1), with the additional subdivision of the population in compartments:

$$\frac{\partial (f_S(\mathbf{x}, \mathbf{v}, t) + f_I(\mathbf{x}, \mathbf{v}, t))}{\partial t} = K_I(f_S, f_I)(\mathbf{x}, \mathbf{v}, t) - K_S(f_S, f_I)(\mathbf{x}, \mathbf{v}, t), \quad (2.9)$$

in which we have renamed

$$\begin{aligned} Q^+(f_S, f_I)(\mathbf{x}, \mathbf{v}, t) &= K_I(f_S, f_I)(\mathbf{x}, \mathbf{v}, t) \\ Q^-(f_S, f_I)(\mathbf{x}, \mathbf{v}, t) &= K_S(f_S, f_I)(\mathbf{x}, \mathbf{v}, t). \end{aligned} \quad (2.10)$$

Splitting the dynamics of susceptible and infected individuals, we resort to the system

$$\begin{aligned} \frac{\partial f_S(\mathbf{x}, \mathbf{v}, t)}{\partial t} &= -K_S(f_S, f_I)(\mathbf{x}, \mathbf{v}, t) \\ \frac{\partial f_I(\mathbf{x}, \mathbf{v}, t)}{\partial t} &= K_I(f_S, f_I)(\mathbf{x}, \mathbf{v}, t). \end{aligned} \quad (2.11)$$

In epidemiological modeling, the functions $K_S(f_S, f_I)$ and $K_I(f_S, f_I)$ are usually known as the local incidence rates, which quantify the transmission of infection. Unlike the classical SIR model, where $K_S = K_I$, due to the presence of the state variable \mathbf{v} , these two functions

take a different form from each other. The function $K_S(f_S, f_I)(\mathbf{x}, \mathbf{v}, t)$ quantifies the amount of individuals that move from the compartment of susceptible people to the compartment of infected people. Linking to (2.3), this is classically done by the expression

$$K_S(f_S, f_I)(\mathbf{x}, \mathbf{v}, t) = f_S(\mathbf{x}, \mathbf{v}, t) \int_{\mathbb{R}_+^4} \kappa(x_2, y_2, w_1) f_I(\mathbf{y}, \mathbf{w}, t) dyd\mathbf{w}. \quad (2.12)$$

According to [15, 16], in (2.12) we set the contact function $\kappa(x_2, y_2, w_1)$ to be a nonnegative function growing both with respect to the social activities x_2, y_2 of the susceptible and infectious individuals, and to degree of infectiousness w_1 of the virus. Moreover the contact function κ is such that $\kappa(x_2, y_2, 0) = \kappa(0, y_2, w_1) = \kappa(x_2, 0, w_1) = 0$, which expresses the fact that the epidemic cannot spread neither in the absence of contagiousness of the virus, nor in the absence of social contact between susceptible and infectious individuals.

A leading example for $\kappa(x, y, w)$ is obtained by choosing, for given positive constants δ, η, θ ,

$$\kappa(x, y, w) = \theta x^\delta y^\delta w^\eta. \quad (2.13)$$

This choice corresponds to take the incidence rate proportional to the product of the number of contacts of susceptible and infected people, and to the infectiousness of the virus. This generalizes a similar choice previously made in [15, 16]. When $\delta = \eta = 1$, for example, the incidence rate takes the simpler form

$$K_S(f_S, f_I)(\mathbf{x}, \mathbf{v}, t) = \theta x_2 f_S(\mathbf{x}, \mathbf{v}, t) \int_{\mathbb{R}_+^4} y_2 w_1 f_I(\mathbf{y}, \mathbf{w}, t) dyd\mathbf{w}. \quad (2.14)$$

As it can be easily argued, the evolution of the epidemic depends heavily on the shape of the function κ used to quantify the rate of possible contagion.

On the other hand, again linking to (2.3), the amount of individuals entering into the infectious compartment is governed by

$$K_I(f_S, f_I)(\mathbf{x}, \mathbf{v}, t) = f_S(\mathbf{x}^*, \mathbf{v}^*, t) \int_{\mathbb{R}_+^4} \kappa(x_2, y_2, w_1) f_I(\mathbf{y}^*, \mathbf{w}^*, t) dyd\mathbf{w}. \quad (2.15)$$

In what follows, to maintain as possible the connection with the methods widely used in classical kinetic theory of rarefied gases, we will often resort to the weak formulation of the contact functions $K_S(f_S, f_I)$ and $K_I(f_S, f_I)$, which corresponds to quantify their action on a given smooth function $\varphi(\mathbf{x}, \mathbf{v})$ (the observable function). Starting from equation (2.12), this leads to the identity

$$\begin{aligned} \int_{\mathbb{R}_+^4} \varphi(\mathbf{x}, \mathbf{v}) K_S(f_S, f_I)(\mathbf{x}, \mathbf{v}, t) d\mathbf{x}d\mathbf{v} = \\ \int_{\mathbb{R}_+^8} \kappa(x_2, y_2, w_1) \varphi(\mathbf{x}, \mathbf{v}) f_S(\mathbf{x}, \mathbf{v}, t) f_I(\mathbf{y}, \mathbf{w}, t) dx dy d\mathbf{v} d\mathbf{w}. \end{aligned} \quad (2.16)$$

Instead, from equation (2.15), after some manipulations typical of kinetic theory related to the change of pre- and post-interaction variables, we obtain

$$\begin{aligned} \int_{\mathbb{R}_+^4} \varphi(\mathbf{x}, \mathbf{v}) K_I(f_S, f_I)(\mathbf{x}, \mathbf{v}, t) d\mathbf{x}d\mathbf{v} = \\ \int_{\mathbb{R}_+^8} \kappa(x_2^*, y_2, w_1) \varphi(\mathbf{x}^*, \mathbf{v}^*) f_S(\mathbf{x}, \mathbf{v}, t) f_I(\mathbf{y}, \mathbf{w}, t) dx dy d\mathbf{v} d\mathbf{w}. \end{aligned} \quad (2.17)$$

We remark that, here, the state vector $(\mathbf{x}^*, \mathbf{v}^*)$ is the post-interaction state of an infected individual which results from the pre-interaction state (\mathbf{x}, \mathbf{w}) , where \mathbf{x} is the socio-physical

condition of the susceptible individual, and \mathbf{w} is the viral impact of the the virus present in the infecting individual responsible for contagion.

Within this picture, we assume that in any new infection the presence of the virus modifies the socio-physical conditions of the susceptible individual, and, at the same time, the viral impact of the new infected individual can be different from the viral impact of the infectious individual responsible for contagion.

It is important to underline that, in presence of a constant observable function φ we have the equality

$$\int_{\mathbb{R}_+^4} K_S(f_S, f_I)(\mathbf{x}, \mathbf{v}, t) d\mathbf{x}d\mathbf{v} = \int_{\mathbb{R}_+^4} K_I(f_S, f_I)(\mathbf{x}, \mathbf{v}, t) d\mathbf{x}d\mathbf{v}, \quad (2.18)$$

which shows that the total number of the population is preserved.

As seen so far, real kinetic dynamics concerns only subjects belonging to the S and I compartments. To also take into account now the mechanism of healing (or death) of infected individuals, we complete the model just introduced according to the SIR dynamics [21], namely according to the system of integro-differential equations

$$\begin{aligned} \frac{\partial f_S(\mathbf{x}, \mathbf{v}, t)}{\partial t} &= -K_S(f_S, f_I)(\mathbf{x}, \mathbf{v}, t) \\ \frac{\partial f_I(\mathbf{x}, \mathbf{v}, t)}{\partial t} &= K_I(f_S, f_I)(\mathbf{x}, \mathbf{v}, t) - \gamma(\mathbf{x}, \mathbf{v})f_I(\mathbf{x}, \mathbf{v}, t) \\ \frac{\partial f_R(\mathbf{x}, \mathbf{v}, t)}{\partial t} &= \gamma(\mathbf{x}, \mathbf{v})f_I(\mathbf{x}, \mathbf{v}, t). \end{aligned} \quad (2.19)$$

Here, the function $\gamma(\mathbf{x}, \mathbf{v}) > 0$ represents the recovery rate, which is assumed to be dependent on the joint action of the personal resistance x_1 of the infected individual and the severity v_2 of the disease. Let us notice that, if both the contact function κ and the recovery rate γ are assumed to be constant, integration of system (2.19) shows that the mass fractions, as given by (2.5), satisfy the classical SIR evolution [21].

In general, the SIR-type model (2.19) is characterized by an *inhomogeneous mixing*. The complete description of the model then requires the knowledge of the binary interaction $(\mathbf{x}, \mathbf{w}) \rightarrow (\mathbf{x}^*, \mathbf{v}^*)$, which characterizes the contagion of a susceptible individual with socio-physical condition \mathbf{x} by an infectious person with viral impact \mathbf{w} , making him/her infected with modified socio-physical condition \mathbf{x}^* and viral impact \mathbf{v}^* . This is an extremely difficult problem which includes, from the point of view of biology, the understanding of the reasons why the dynamics at the molecular scale leads to an evolution in time of the biological features of the virus up to mutations, and how these affects the in-host consequences of the presence of the virus. Having this behavior in mind, in a largely arbitrary manner we will hypothesize that both individual and virus behavior are driven by utility reasons, mainly related to their survival. Once this hypothesis has been fixed, a well-known interaction rule which is based on utility functions can be identified in the Edgeworth box, of common use in economics. Since this argument is maybe not so well known by people working in compartmental epidemiology, we will briefly present it in the next Section.

3 Virus-agent interaction based on mutual utility

The aim of this Section is to briefly discuss a framework for the binary interaction characterizing the contagion of a susceptible individual, which is derived directly from the basic principles of economics. To this aim we will first review the classical Edgeworth box theory of economic transactions. Next we will describe how the same principles can be applied in the virus-agent interactions.

3.1 Edgeworth box and Cobb-Douglas utility function

People exchange goods. The advantages they obtain are contingent upon the extent and conditions of their exchange. This important question is attempted to be answered by price theory. A binary transaction might involve a wide range of trades, some of which would be preferred by one party over the other but all of which would be advantageous to both. In the following, we will assume that the agents inside the system own the same two kinds of goods and that there is no production, meaning that the overall quantity of goods stays constant. If (x_A, y_A) and (x_B, y_B) denote the quantity of goods of two agents A and B , respectively, then

$$p_A = \frac{x_A}{x_A + x_B}, \quad q_A = \frac{y_A}{y_A + y_B} \quad (3.20)$$

are the percentages of goods of the first agent. As a matter of definitions, the point (p_A, q_A) belongs to the square $\mathcal{S} = [0, 1] \times [0, 1]$.

To provide a foundation for the motivations behind trading, conventional wisdom holds that an agent's actions are determined by its utility function. The *Cobb-Douglas utility function* is among the most often used of these functions:

$$U_{\alpha, \beta}(p, q) = p^\alpha q^\beta, \quad \alpha + \beta = 1. \quad (3.21)$$

Each agent aims to optimize its individual satisfaction through trade. The parameters α and β are associated with the preferences an agent attributes to the two goods. When $\alpha > \beta$, the agent has a preference for acquiring goods of the first type (designated by x). If $\alpha = \beta = 0.5$, it is evident that both goods hold equal importance for agent A . Given the percentage point (p_A, q_A) of agent A , the curve

$$U_{\alpha, \beta}(p, q) = U_{\alpha, \beta}(p_A, q_A)$$

denotes the *indifference curve* for agent A . In fact, any point on the indifference curve yields the same level of utility for agent A . It is important to observe that the indifference curve for A lies entirely within set \mathcal{S} and divides the square into two distinct regions:

$$U_A^- = \{(p, q) : U_{\alpha, \beta}(p, q) < U_{\alpha, \beta}(p_A, q_A)\},$$

$$U_A^+ = \{(p, q) : U_{\alpha, \beta}(p, q) > U_{\alpha, \beta}(p_A, q_A)\}.$$

Evidently, any trade that shifts the proportions of agent A into the region U_A^+ will enhance the utility function and be deemed acceptable by the agent.

In the scenario of a binary trade, agent B also possesses a Cobb-Douglas utility function with preference parameters generally distinct from those of agent A . Similarly, there exists an indifference curve for agent B and a specific region where the utility of B increases post-trade. Ultimately, a trade becomes acceptable for both agents when their respective percentages of goods after the trade fall within the regions where both utility functions experience an increase.

An insightful perspective on such a scenario is offered by the Edgeworth Box, named after Francis Y. Edgeworth, the author of the 19th-century work *Mathematical Psychics* [17]. The Edgeworth box is constructed by rotating the square \mathcal{S} where the indifference curve of agent B is delineated by 180° around the center of the square $(0.5, 0.5)$ and by considering the indifference curve of agent A and the rotated indifference curve of B together on the same square (see Figure 3.2 for an example).

Any point within the Edgeworth box represents a potential distribution of the total quantities of A and B , where the share of A is measured from the lower left-hand corner, and the share of B is measured from the upper right-hand corner. Each conceivable trade corresponds to a transition from one point in the box to another.

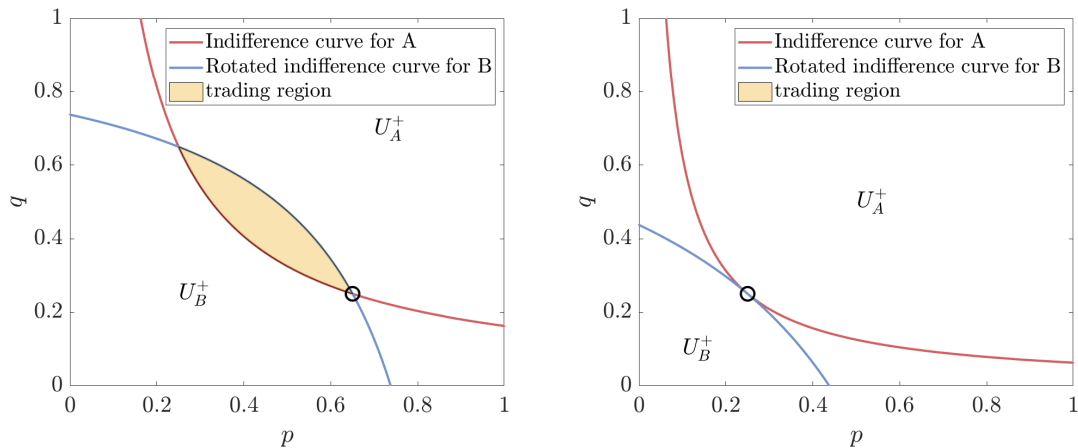


Figure 3.2: Edgeworth box. Indifference curves in a binary trade for the Cobb-Douglas utility function (3.21) with $\alpha = \beta = 0.5$. On the left, the trading region for $(p_A, q_A) = (0.65, 0.25)$ (and, therefore, $(p_B, q_B) = (0.35, 0.75)$), indicated with the black circle; on the right, there is a unique tangency point (Pareto optimal) at $(p_A, q_A) = (0.25, 0.25)$.

By design, given the jointly concave nature of the Cobb-Douglas utility function, the utility of A increases when the point shifts up and to the right, while the utility of B increases when the point moves down and to the left. The specific region where this occurs is precisely the overlapping area between U_A^+ and U_B^+ , rotated by 180° .

The operational approach to trading facilitated by the Edgeworth box yields intriguing implications. When the percentages of A and B allow for a potential trading region, the completion of a trade causes the point to shift within the region, subsequently reducing the scope of the new trading area. If both agents intelligently select a point within the region where the two indifference curves are tangent, indicating a point of maximum mutual satisfaction, any movement from this point towards a higher indifference curve for one agent corresponds to a lower curve for the other. Consequently, any trade that benefits one agent harms the other. The points where the two curves are tangent are not unique, and the collection of points from which no further mutually beneficial trading is feasible, known as *Pareto optimal* points, constitutes the *contract curve*. The contract curve has a connection to prices. At the point of tangency between the two indifference curves, the slope of the tangency line denotes the relative prices of the two goods. Therefore, there exist relative prices consistent with Pareto optimality, and these prices maximize the potential budget for both agents.

A kinetic model of Boltzmann type, with binary interactions based on Edgeworth box, has been presented and discussed in [29]. In this model, a key aspect is the presence of randomness in the trade, motivated by the incomplete knowledge of the market.

3.2 A viral interaction model

Mutatis mutandis, the modeling assumptions in [29] can be fruitfully applied to construct a *viral* interaction between the pair of susceptible and infected individuals, based on mutual utility.

Let S , respectively I , denote a susceptible, respectively infectious, individual, which are identified by the pair (\mathbf{x}, \mathbf{w}) of the socio-physical conditions \mathbf{x} of S and the viral impact \mathbf{w} of I . In what follows, we assume that the individual S and the virus present in I exhibit the same type of utility function (3.21), but in general with different preferences. We assume

moreover that the preferences of S are determined by the search of its own best socio-physical conditions, while the preferences of the virus present in I are linked to its survival. We outline that possible heterogeneity in individuals' preferences is neglected in our model, an acceptable simplification because all individuals are exposed to similar risk. Likewise, we neglect possible heterogeneity in virus preferences. Clearly, in both classes, preferences can be assumed to vary with time without any additional difficulty in modeling.

Before entering into the detail of the interaction, let us fix some points that allow to better identify the various parameters characterizing the *virus-agent* Edgeworth box. It is reasonable to assume that the evolutionary choice of the virus goes toward increasing contagiousness (w_1), since high contagiousness ensures its survival. Conversely, individuals will aim at maintaining a higher level of survival rate (x_1). Therefore, the higher the contagiousness of the virus, the more the disease resistance (survival rate) of the susceptible individual will decrease, and vice versa. Additionally, we can assume that the individual behavior, and the consequent evolutionary preferences, are heavily dependent on the state of the epidemic spread. This can be expressed by hypothesizing that in presence of a high degree of virus severity (w_2), individuals' sociality tends to be reduced by them (x_2), while the opposite effect occurs in light of a low degree of severity, since in this case the risks associated with social activity are perceived as low.

According to this discussion, it seems appropriate to relate the pairs *resistance-contagiousness* and *sociality-severity*, which are associated to something similar to a conservation law, namely that the quantities *resistance+contagiousness* and *sociality+severity* are invariants of the interaction, and, furthermore, that they are related to similar degrees of preferences. In this sense, during the evolutionary dynamics, when one variable decreases, its pair counterpart increases, and vice-versa. Thus, the Edgeworth box pair (p_S, q_S) of the susceptible individual is defined by

$$p_S = \frac{x_1}{x_1 + w_1}, \quad q_S = \frac{x_2}{x_2 + w_2}, \quad (3.22)$$

while the pair (p_I, q_I) of the virus in any infected individual is

$$p_I = \frac{w_1}{x_1 + w_1}, \quad q_I = \frac{w_2}{x_2 + w_2}. \quad (3.23)$$

To proceed, it is necessary to explicitly identify a possible virus-agent interaction that leads to an increase in the utility functions of both. The underlying idea is that the time evolution of the solution of the system (2.19) is essentially characterized by the fact that the elementary interactions lead to the growth of the Cobb-Douglas utility functions. To this aim, we extend the analysis of [29] to the case where the individuals are endowed with different preferences.

Following the analysis in [29], if an individual, denoted by A , has percentages p and q and preferences (α, β) , with $\alpha + \beta = 1$, in its Edgeworth box, we assume that the interactions are characterized by the movements of the point (p, q) into $(p^*, q^*) \in \mathcal{S}$, where

$$\begin{aligned} p^* &= p + \mu\beta(q - p) \\ q^* &= q + \tilde{\mu}\alpha(p - q). \end{aligned} \quad (3.24)$$

We remark that in this case the variation of the position (p, q) of the individual is fully characterized by its own preferences. In (3.24) μ and $\tilde{\mu}$ are nonnegative random variables with mean $\lambda > 0$ and finite variance. We will assume moreover that

$$\mu\beta < 1, \quad \tilde{\mu}\alpha < 1. \quad (3.25)$$

Under this condition, the post-interaction point (p^*, q^*) belongs to \mathcal{S} , and it is an admissible point for the Edgeworth box. It is immediate to show that, unless $p = q$, and in absence of

randomness, that is if the pair (p^*, q^*) is given by

$$\begin{aligned} p^* &= p + \lambda\beta(q - p) \\ q^* &= q + \lambda\alpha(p - q), \end{aligned} \quad (3.26)$$

the interaction, for $\lambda < 1$, increases the Cobb-Douglas utility function of the individual. Indeed, for $\lambda < 1$, a simple computation gives [29]

$$\frac{d}{d\lambda} U_{\alpha,\beta}(p^*, q^*) = \alpha\beta(1 - \lambda)(p - q)^2(p^*)^{\alpha-1}(q^*)^{\beta-1} > 0. \quad (3.27)$$

Hence, if both individuals share the same preferences, interactions of type (3.24) increase the utilities of both.

Let us now suppose that a second individual, denoted by B , has preferences (α_1, β_1) , with $\alpha_1 + \beta_1 = 1$, and $\alpha_1 \neq \alpha$, hence $\beta_1 \neq \beta$. Suppose moreover that

$$\frac{\alpha}{\beta} < \frac{\alpha_1}{\beta_1}. \quad (3.28)$$

At difference with the previous case, we consider as possible interactions of the individual A also the movements of the point (p, q) into $(p_1^*, q_1^*) \in \mathcal{S}$, where

$$\begin{aligned} p_1^* &= p + \mu\beta_1(q - p) \\ q_1^* &= q + \tilde{\mu}\alpha_1(p - q). \end{aligned} \quad (3.29)$$

In this case, the variation of the position (p, q) of the individual A is influenced by the preferences of the individual B . For the sake of simplicity, we assume that the randomness in (3.29) is determined by the same random variables μ and $\tilde{\mu}$ appearing in (3.24), further satisfying

$$\mu\beta_1 < 1, \quad \tilde{\mu}\alpha_1 < 1, \quad (3.30)$$

so that the post-interaction point (p_1^*, q_1^*) belongs to \mathcal{S} . Different choices of the random effects could be considered, at the price of an increasing rate of computations.

In absence of randomness, the pair (p_1^*, q_1^*) associated to (3.29) is given by

$$\begin{aligned} p_1^* &= p + \lambda\beta_1(q - p) \\ q_1^* &= q + \lambda\alpha_1(p - q). \end{aligned} \quad (3.31)$$

In correspondence to interaction (3.31), one obtains

$$\begin{aligned} \frac{d}{d\lambda} U_{\alpha,\beta}(p_1^*, q_1^*) &= (p_1^*)^{\alpha-1}(q_1^*)^{\beta-1} \left\{ (\beta - \beta_1\lambda)\alpha_1 p^2 + \right. \\ &\quad \left. (\alpha - \alpha_1\lambda)\beta_1 q^2 + 2 \left[\alpha_1\beta_1\lambda - \frac{1}{2}(\alpha\beta_1 + \beta\alpha_1) \right] pq \right\}. \end{aligned} \quad (3.32)$$

Let λ satisfy the condition

$$\lambda \leq \frac{\alpha}{\alpha_1}, \quad (3.33)$$

so that, in view of (3.28), $\lambda < \beta/\beta_1$, and let us set $x = p/q$. Under condition (3.33), the second-degree polynomial

$$(\beta - \beta_1\lambda)\alpha_1 x^2 + 2 \left[\alpha_1\beta_1\lambda - \frac{1}{2}(\alpha\beta_1 + \beta\alpha_1) \right] x + (\alpha - \alpha_1\lambda)\beta_1$$

is nonnegative if and only if x lies outside the interval of the two roots x_1 and x_2 , which are given by

$$x_1 = \frac{(\alpha - \alpha_1 \lambda) \beta_1}{(\beta - \beta_1 \lambda) \alpha_1}, \quad x_2 = 1.$$

Since (3.28) holds, $0 < x_1 < x_2$. Hence, for all values of λ satisfying (3.33), the utility function $U_{\alpha, \beta}(p_1^*, q_1^*)$ is nondecreasing in the half-square $p \geq q$.

Thus, if (3.28) holds, and $p \geq q$, for any given λ satisfying (3.33),

$$U_{\alpha, \beta}(p_1^*, q_1^*) \geq U_{\alpha, \beta}(p, q), \quad U_{\alpha_1, \beta_1}(1 - p_1^*, 1 - q_1^*) \geq U_{\alpha_1, \beta_1}(1 - p, 1 - q),$$

and the utility functions of both individuals are nondecreasing.

The previous computations can be repeated in the half-square $p \leq q$ with the interaction (3.26), and utility function $U_{\alpha_1, \beta_1}(p^*, q^*)$. In this case, provided λ satisfies the bound

$$\lambda \leq \frac{\beta_1}{\beta}, \tag{3.34}$$

so that, in view of (3.28), $\lambda < \alpha_1/\alpha$, the utility functions of both individuals are nondecreasing.

Hence, joining the two results, we conclude that, in absence of randomness, for any given pairs of preferences such that (3.28) holds, and for any λ such that

$$\lambda \leq \min \left\{ \frac{\alpha}{\alpha_1}, \frac{\beta_1}{\beta} \right\}, \tag{3.35}$$

the interaction defined by (3.26) in the half-square $p \leq q$ (respectively (3.31) in the half-square $p \geq q$), is such that the Cobb-Douglas utility functions of both individuals are nondecreasing.

The just described interaction refers to the purely theoretical situation in which the individual knows all about the interaction and its result. In general, this is not realistic, and it appears reasonable to postulate that the result of the interaction has a share of unpredictability, so that increasing of utility can be assumed only in the mean. If one agrees with this, then interactions of type (3.24) satisfy all constraints of Edgeworth box, but the single interaction can move the point in a region which is convenient only for one of the two interacting agents, as well as in the region which is not convenient for both.

Let $I_E(x)$ denote the characteristic function of the set E , namely the function such that

$$I_E(x) = 1 \quad \text{if } x \in E; \quad I_E(x) = 0 \quad \text{if } x \notin E.$$

Then, if we define

$$\Psi_\lambda(a, b, p, q) = \lambda [aI_{\{p < q\}} + bI_{\{p > q\}}], \tag{3.36}$$

we assume that the Cobb-Douglas increasing interaction characterizing the pairs of preferences (α_S, β_S) and (α_I, β_I) is given by

$$\begin{aligned} p^* &= p + \Psi_\mu(\beta_S, \beta_I, p, q)(q - p) \\ q^* &= q + \Psi_{\tilde{\mu}}(\alpha_S, \alpha_I, p, q)(p - q), \end{aligned} \tag{3.37}$$

The interaction (3.37) is further characterized by the random variables μ and $\tilde{\mu}$ of mean λ satisfying (3.35), and such that both (3.25) and (3.30) hold.

Going back to the object of our analysis, the interaction modifies the pairs (p_S, q_S) , (p_I, q_I) of the susceptible individual and, respectively, of the virus according to

$$\begin{aligned}
p_S^* &= p_S + \Psi_\mu(\beta_S, \beta_I, p_S, q_S)(q_S - p_S) \\
q_S^* &= q_S + \Psi_{\bar{\mu}}(\alpha_S, \alpha_I, p_S, q_S)(p_S - q_S) \\
p_I^* &= p_I + \Psi_\mu(\beta_I, \beta_S, p_I, q_I)(q_I - p_I) \\
q_I^* &= q_I + \Psi_{\bar{\mu}}(\alpha_I, \alpha_S, p_I, q_I)(p_I - q_I).
\end{aligned} \tag{3.38}$$

Note that the post-interaction values in (3.38) satisfy the obvious relations

$$p_S^* + p_I^* = q_S^* + q_I^* = 1,$$

which guarantee that the post-interaction values are percentage values split between S and I , like in (3.22) and (3.23).

Moreover, note that the knowledge of the percentages p_S^* and p_I^* (respectively q_S^* and q_I^*) does not allow to recover uniquely the post-interaction values $(\mathbf{x}^*, \mathbf{w}^*)$, since the relations (3.22) and (3.23) admit infinite solutions. However, assuming the constraints $x_1 + w_1 = x_1^* + w_1^*$ and $x_2 + w_2 = x_2^* + w_2^*$, we obtain that the interaction between the individual in S with state \mathbf{x} and preferences (α_S, β_S) and the virus in I with state \mathbf{w} and preferences (α_I, β_I) is given by

$$\begin{aligned}
x_1^* &= x_1 + \Psi_\mu \left(\beta_S, \beta_I, \frac{x_1}{x_1 + w_1}, \frac{x_2}{x_2 + w_2} \right) \left(\frac{x_1 + w_1}{x_2 + w_2} x_2 - x_1 \right) \\
x_2^* &= x_2 + \Psi_{\bar{\mu}} \left(\alpha_S, \alpha_I, \frac{x_1}{x_1 + w_1}, \frac{x_2}{x_2 + w_2} \right) \left(\frac{x_2 + w_2}{x_1 + w_1} x_1 - x_2 \right) \\
w_1^* &= w_1 + \Psi_\mu \left(\beta_I, \beta_S, \frac{w_1}{x_1 + w_1}, \frac{w_2}{x_2 + w_2} \right) \left(\frac{x_1 + w_1}{x_2 + w_2} w_2 - w_1 \right) \\
w_2^* &= w_2 + \Psi_{\bar{\mu}} \left(\alpha_I, \alpha_S, \frac{w_1}{x_1 + w_1}, \frac{w_2}{x_2 + w_2} \right) \left(\frac{x_2 + w_2}{x_1 + w_1} w_1 - w_2 \right).
\end{aligned} \tag{3.39}$$

The process just described clearly follows an evolutionary dynamic between the virus (in the infected individual) and the susceptible agent that traces the Cobb–Douglas mechanism of continuous mutual utility. In fact, the post-interaction quantities in (3.39) are related to the pre-interaction quantities by nonlinear relationships such that, at least on average, the Cobb–Douglas utility functions of both individuals increase: both the susceptible individual and the virus evolve by pursuing their own (distinct) interests. From a purely epidemiological point of view, it is spontaneous to assume that the advantages gained by the virus in each evolutionary step do not manifest themselves in the updating of the \mathbf{w} utility variables proper to the I individual, but rather in an activation of the viral variables of the S subject. The latter, in fact, as a result of the interaction with I (with virus that has followed an evolution that wishes to increase its contagiousness and severity) becomes the recipient of the increased utility share gained from the evolutionary process, expressed in terms of viral impact. Thus, considering an interaction between $f_S(\mathbf{x}, \mathbf{v}, t)$, with $\mathbf{v} = \mathbf{0}$, and $f_I(\mathbf{y}, \mathbf{w}, t)$ we compute the updates $\mathbf{x} \rightarrow \mathbf{x}^*$ and $\mathbf{v} \rightarrow \mathbf{v}^* = \mathbf{w}^*$ as in (3.39), while both socio-physical condition \mathbf{y} and viral impact \mathbf{w} of the agent I remain unchanged at the end of the interaction. A sketch of this process is shown in Figure 3.3. This modeling choice finds its rationale also when observing that an infected individual does not tend to acquire greater infectiousness or severity on its own after an interaction with a susceptible; rather, the increase in viral disease characteristics occurs at the level of the interacting pair, with the susceptible becoming infected by activation of its viral load.

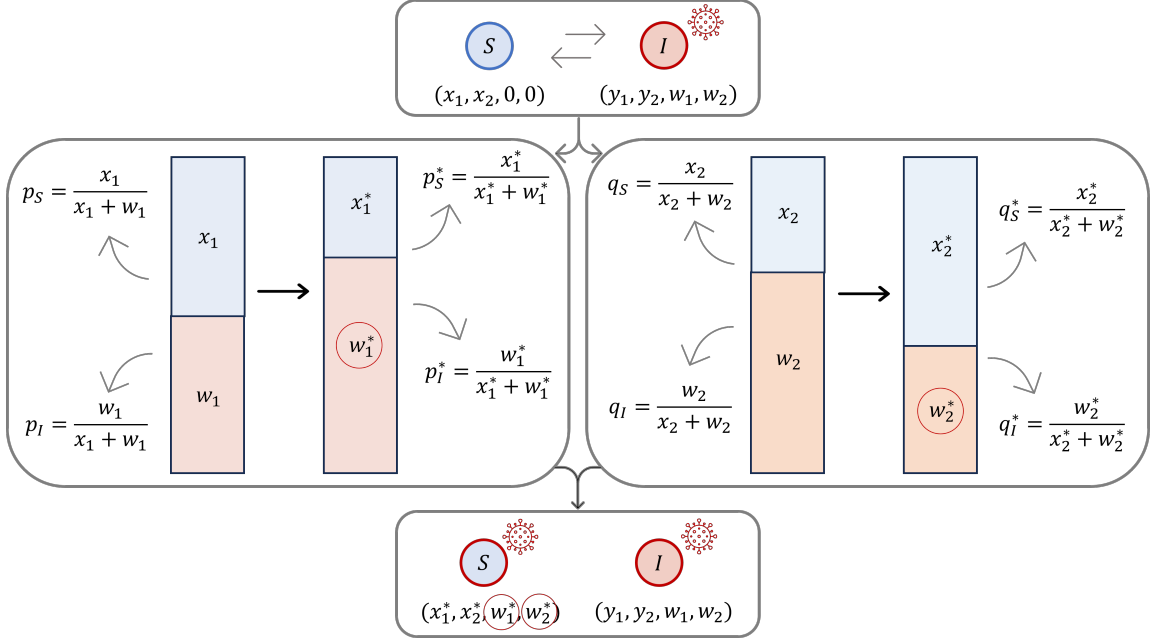


Figure 3.3: Sketch of the interaction between the pair of susceptible (S) and infected (I) individuals (*virus-agent* interaction) based on mutual utility with respect to the invariants *resistance+contagiousness* ($x_1 + w_1$) and *sociality+severity* ($x_2 + w_2$). The post-interaction socio-physical and viral states, (x_1^*, x_2^*) and (w_1^*, w_2^*) , respectively, are both acquired at the level of the susceptible state update, whereas the pre-infected individual I does not undergo a change of state.

Remark 3.1 *Interaction (3.24) is only one of the possible interactions which lead to an increased utility, but many others can be considered. However, interactions of type (3.24) have the interesting property to be linear in the percentage values entering into the Edgeworth box, and to furnish explicit values for the interactions which lead to the correct convenient area for both interacting agents. This will be enough to perform a numerical study of the evolution in time of the guest-virus pandemic.*

4 Numerical tests

To show the validity of the proposed model, we perform several numerical experiments employing one of the most commonly used Monte Carlo methods for the simulation of the interaction operators (2.10), namely Nanbu-Babovsky's scheme. For the detailed algorithm the reader can refer to [26, 27]. To numerically solve the complete SIR system (2.19), we apply a classical splitting procedure, for which the interaction operator and the recovery process are solved in sequence [27].

Test 1. In the first numerical test we consider a population of $N = 10^5$ individuals in which at the beginning of the simulation there is only 1 infected agent, while the rest are susceptible. We define the same preference coefficients for all S and I agents, fixing $\alpha_S = \alpha_I = \beta_S = \beta_I = 0.5$, and characterizing the uniformly distributed random variables μ and $\tilde{\mu}$ with the same mean $\lambda = 0.99$, satisfying (3.35), and same variance equal to 0.01. We adopt a simple setting in which the interaction kernel is constant, choosing first $\kappa = 1$ (case a) and then $\kappa = 0.5$ (case b), and we perform both test cases in two different configurations: considering the simplest possible compartmentalization of only S and I agents (thus omitting the healing

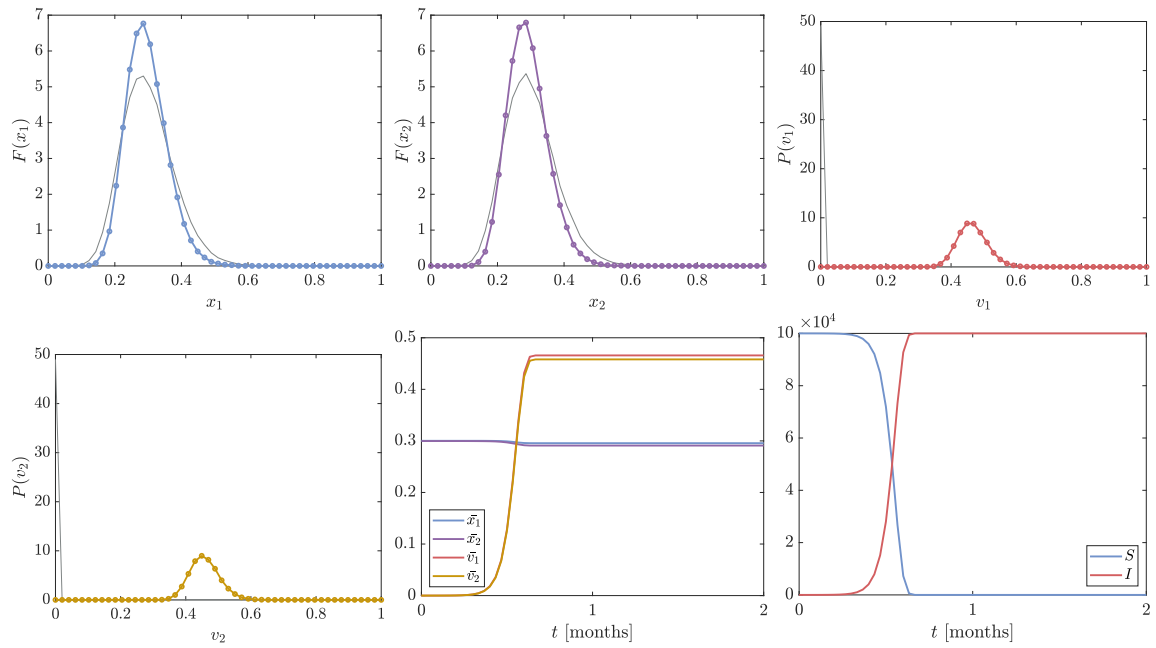


Figure 4.4: Test 1(a), SI-type. Form left to right, top to bottom: distribution of the state variables x_1 (resistance to the disease), x_2 (sociality), v_1 (contagiousness of the virus) and v_2 (severity of the virus) in the whole population at the final time $T = 60$ days in colors and at the initial time in gray; temporal evolution of the mean value of each state variable; evolution in time of the S and I compartments.

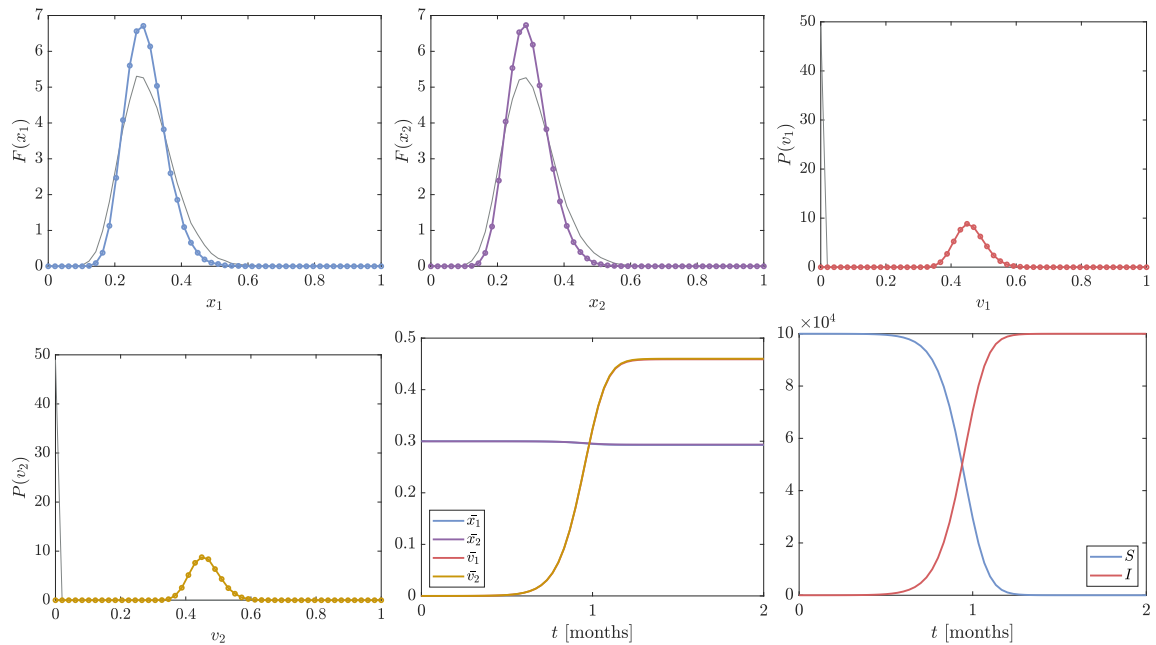


Figure 4.5: Test 1(b), SI-type. Form left to right, top to bottom: distribution of the state variables x_1 (resistance to the disease), x_2 (sociality), v_1 (contagiousness of the virus) and v_2 (severity of the virus) in the whole population at the final time $T = 60$ days in colors and at the initial time in gray; temporal evolution of the mean value of each state variable; evolution in time of the S and I compartments.

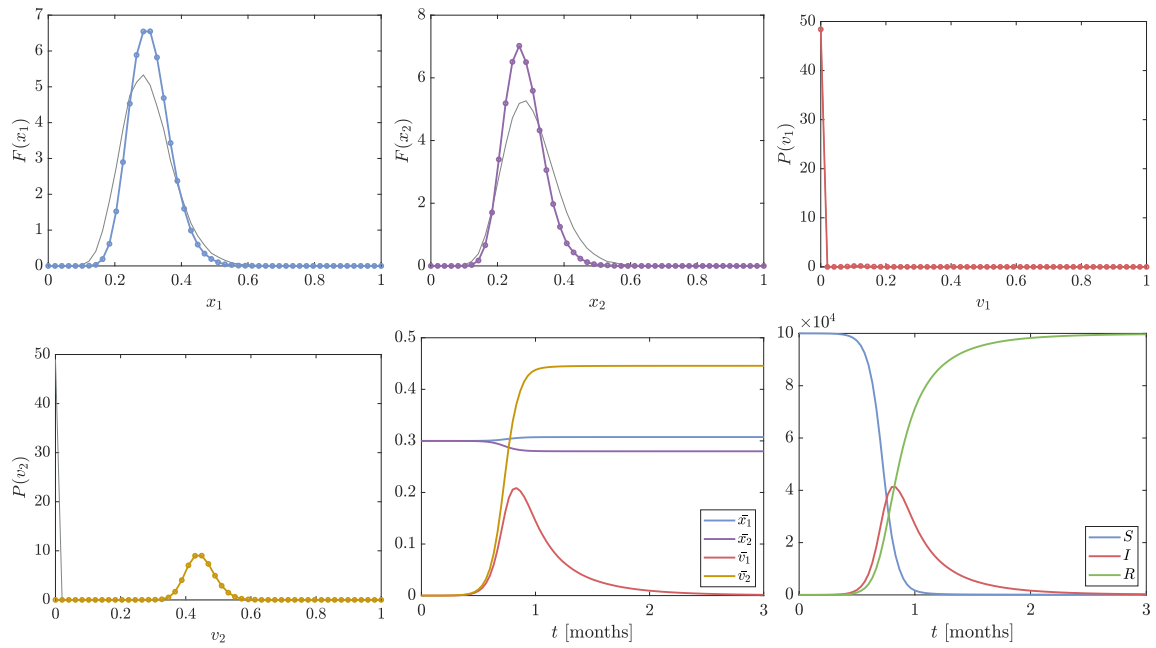


Figure 4.6: Test 1(a), SIR-type. Form left to right, top to bottom: distribution of the state variables x_1 (resistance to the disease), x_2 (sociality), v_1 (contagiousness of the virus) and v_2 (severity of the virus) in the whole population at the final time $T = 90$ days in colors and at the initial time in gray; temporal evolution of the mean value of each state variable; evolution in time of the S, I and R compartments.

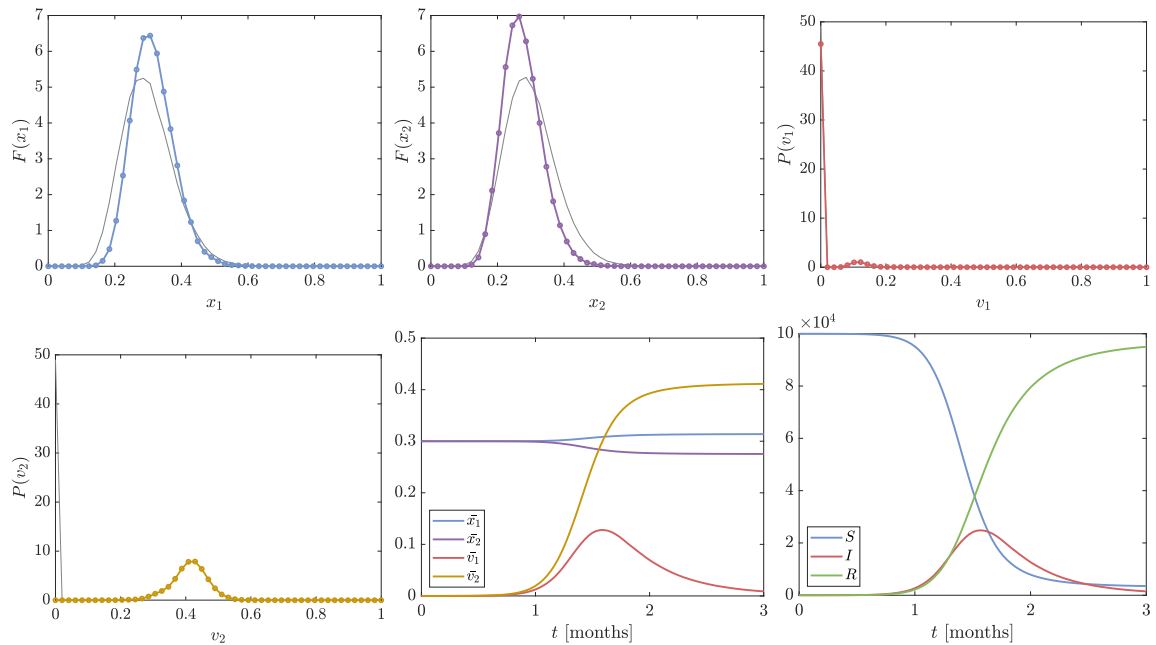


Figure 4.7: Test 1(b), SIR-type. Form left to right, top to bottom: distribution of the state variables x_1 (resistance to the disease), x_2 (sociality), v_1 (contagiousness of the virus) and v_2 (severity of the virus) in the whole population at the final time $T = 90$ days in colors and at the initial time in gray; temporal evolution of the mean value of each state variable; evolution in time of the S, I and R compartments.

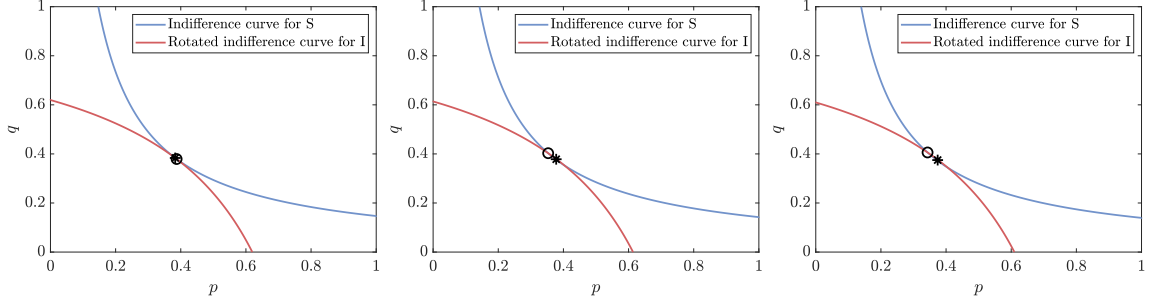


Figure 4.8: Test 1(b), SIR-type. Infectious dynamics in the Edgeworth box at $t = 1$, $t = 45$, $t = 90$ days (from left to right) averaged for all interactions that occurred at that time instant between the S-I pairs. The circle indicates the state pre-interaction, while the star depicts the state post-interaction.

process) and, later, considering the classical SIR-type one, with $\gamma(\mathbf{x}, \mathbf{v}) = 10^{-1} v_2/x_1$ days $^{-1}$. For all the simulations we fix the same initial distributions for the state variables \mathbf{x} and \mathbf{v} . We consider a gamma distribution with shape and scale parameter respectively equal to 3 and 1, rescaled by a factor of 0.1, for both the socio-physical conditions \mathbf{x} , and we attribute a random value of viral impact states \mathbf{v} to the single infected agent following a Gaussian distribution with mean 0.4 and variance 0.01. We run the simulation up to the final time $T = 60$ days in the case of the SI configuration and $T = 90$ days in the SIR one. We fix $\Delta t = 1$ day, respecting the CFL stability condition of the method (see [27]).

For each combination of cases, the average values resulting from 5 stochastic runs are shown in Figures 4.4-4.7. It is immediate to observe, first of all, that the proposed methodology is able to recover the standard SI and SIR-type evolutions of the infectious disease by looking at the bottom-right plot of each Figure. In addition, it is possible to see what is the effect of the different choice of interaction kernel. Indeed, the halving of κ leads to a significant slowdown in the spread of the virus, as expected. The halving of κ , in fact, implies that there is only a 50% chance (and no longer a 100% chance) that a susceptible individual will become infected when it comes in contact with the infected agent. Finally, in the same figures it is possible to appreciate the variation in the distribution of the state variables as well as the evolution of their mean value over time, noting that even choosing $\alpha_S = \beta_S = 0.5$, the SIR dynamics leads to a different final mean for x_1 and x_2 , favoring x_1 (survival rate to the disease).

Finally, in Figure 4.8 we present the dynamics of Test 1b, with SIR compartments, from the perspective of the Edgeworth box at 3 different time steps ($t = 1$, $t = 45$, $t = 90$ days) averaged for all interactions that occurred at that time instant between the S-I pairs. We can observe that in all instances we are almost at the Pareto optimal.

Test 2. In the second numerical test, we stick directly to the SIR compartments and consider a population of $N = 10^4$ individuals among which 1% are initially infected. We then assign different preference coefficients to the S and I subpopulations, choosing $\alpha_S = 0.7$, $\alpha_I = 0.4$ (hence, $\beta_S = 0.3$, $\beta_I = 0.6$). As previously done, we characterize both the uniformly distributed random variables μ and $\tilde{\mu}$ with mean $\lambda = 0.49$ and variance 0.01. Moreover, we consider an initial gamma distribution with shape and scale parameter respectively equal to 3 and 1, rescaled by a factor of 0.1, for both the socio-physical conditions \mathbf{x} , and we attribute a random value of viral impact states \mathbf{v} to the initially infected agents following a Gaussian distribution with mean 0.4 and variance 0.01. In contrast with the previous test, in this one we define a non-constant interaction kernel. Following (2.13), we set $\kappa(x_2, y_2, w_1) = \theta x_2^\delta y_2^\delta w_1^\eta$ with $\theta = 2$ and $\delta = \eta = 1$. The recovery rate is fixed to be $\gamma(\mathbf{x}, \mathbf{v}) = 14^{-1} v_2/x_1$ days $^{-1}$. We

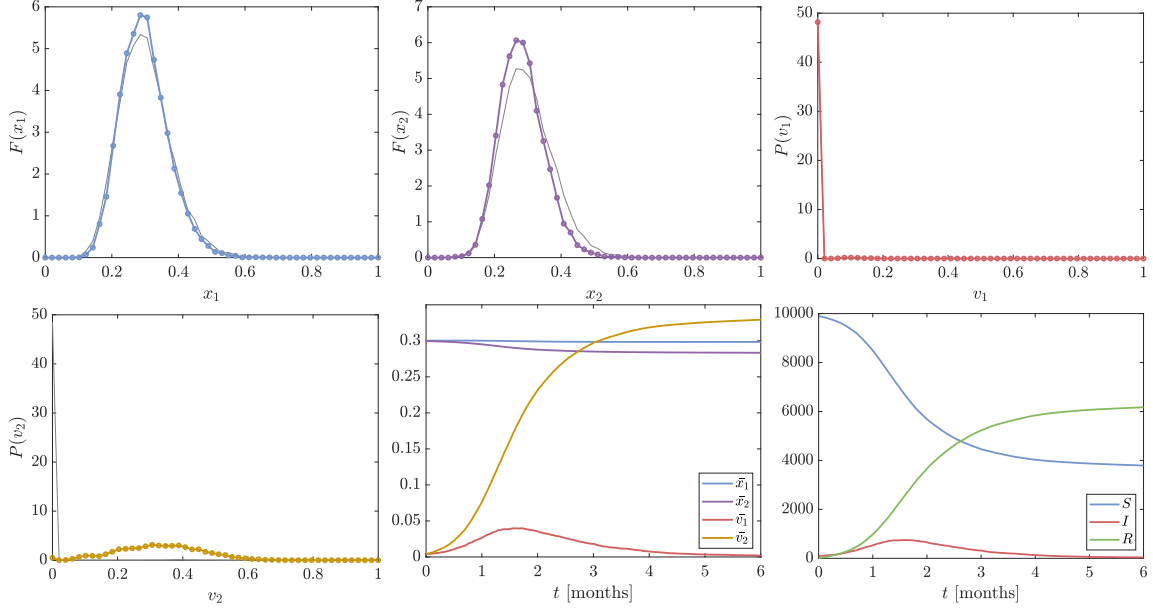


Figure 4.9: Test 2. From left to right, top to bottom: distribution of the state variables x_1 (resistance to the disease), x_2 (sociality), v_1 (contagiousness of the virus) and v_2 (severity of the virus) in the whole population at the final time $T = 180$ days in colors and at the initial time in gray; temporal evolution of the mean value of each state variable; evolution in time of the S , I and R compartments.

run the simulation up to the final time $T = 180$ days with $\Delta t = 1/4$ of a day. In practice, with this choice, a single agent is assumed to interact 4 times with another random individual over the course of a day.

We present the average values resulting from 5 stochastic runs in Figure 4.9. Here it is possible to observe that the chosen interaction kernel leads to a consistent containment of the spread of the virus with respect to the case of Test 1, making the evolution of the dynamics much less predictable. Also the choice of different preference coefficients α and β enriches the dynamics and leads to a necessary reduction of the λ value, due to the restriction (3.35) given by the Cobb-Douglas utility function, playing a significant role in the infectious process.

Test 3. In the last test, we consider again a population of $N = 10^4$ individuals among which 1% are initially infected, but exploring the effects of preference coefficients α and β that are variable in time, simulating a sort of seasonal trends of these parameters. Thus, we define

$$\alpha_S(t) = \beta_I(t) = 0.5 + 0.4 \cos\left(\frac{2\pi t}{T}\right) \quad \alpha_I(t) = \beta_S(t) = 0.5 - 0.4 \cos\left(\frac{2\pi t}{T}\right),$$

with $T = 1$ year. With this choice, we are hypothesizing that during the spring-summer season individuals will tend to prefer sociality over disease resistance, while, in the same time frame, the virus will tend to favor contagiousness over severity. As a consequence, also the coefficient $\lambda := \lambda(t)$, varying in time while respecting restriction (3.35).

In addition, in this test we introduce the dynamics of loss of immunity, considering that a healed individual will lose immunity to the virus 2 months after his/her recovery. This dynamic, at the modeling level, is introduced in a manner entirely similar to that of healing. Hence, the loss of immunity rate is fixed to be $\sigma(\mathbf{x}, \mathbf{v}) = 60^{-1} x_1/v_2$ days $^{-1}$. We consider

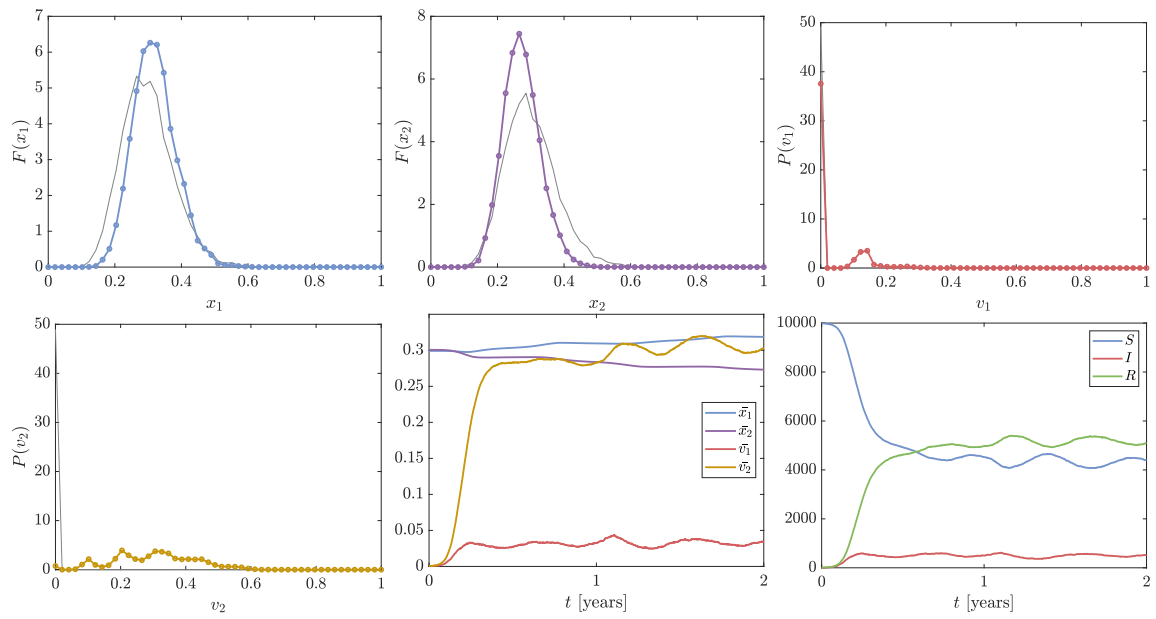


Figure 4.10: Test 3(a). Form left to right, top to bottom: distribution of the state variables x_1 (resistance to the disease), x_2 (sociality), v_1 (contagiousness of the virus) and v_2 (severity of the virus) in the whole population at the final time $2T = 2$ years in colors and at the initial time in gray; temporal evolution of the mean value of each state variable; evolution in time of the S , I and R compartments.

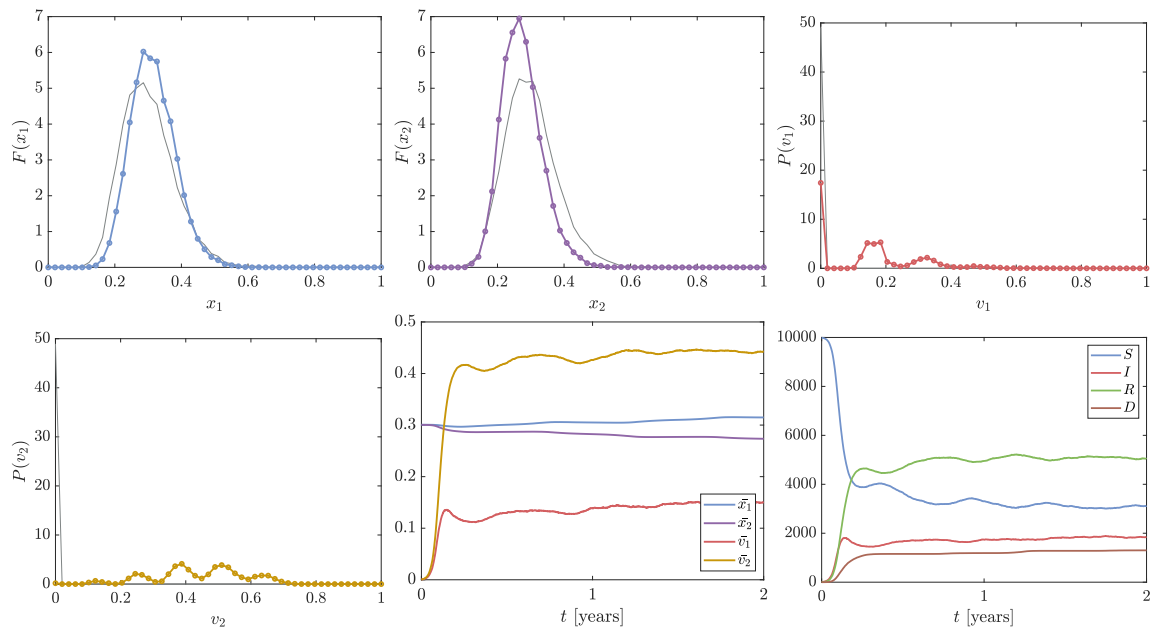


Figure 4.11: Test 3(b). Form left to right, top to bottom: distribution of the state variables x_1 (resistance to the disease), x_2 (sociality), v_1 (contagiousness of the virus) and v_2 (severity of the virus) in the whole population at the final time $2T = 2$ years in colors and at the initial time in gray; temporal evolution of the mean value of each state variable; evolution in time of the S , I , R and D compartments.

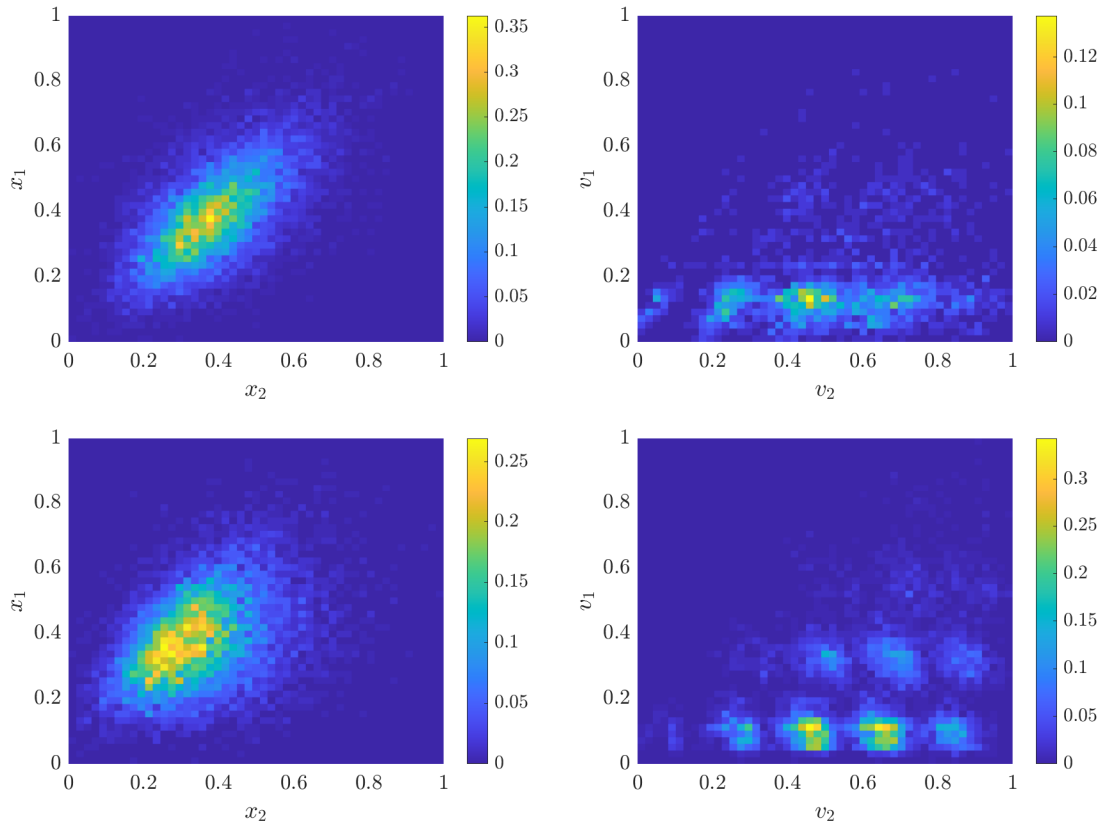


Figure 4.12: Test 3. Bivariate distribution of socio-physical condition (left) and viral impact (right) at the final time for test case (a) (first row) and case (b) (second row). The viral impact is presented taking into account only the contribution of infected agents.

two different configurations: in Test 3(a), the rest of the parameters, including the initial conditions, are left unchanged from Test 2; in Test 3(b), we simulate the spread of a more severe virus by changing the initial distribution of the variables \mathbf{v} , this time following a Gaussian with mean 0.6 (instead of 0.4), and we increase the mean time to recovery to 20 days (i.e., $\gamma(\mathbf{x}, \mathbf{v}) = 20^{-1} v_2/x_1$ days $^{-1}$). Furthermore, as mentioned in Section 2.2, we introduce the process of death by setting an upper limit of severity $v_2 = 0.75$ beyond which the individual is considered deceased. This approach essentially allows us to introduce an additional D compartment of deceased individuals into the model. Both simulations are performed up to $2T = 2$ years, again fixing $\Delta t = 1/4$ of a day.

We present the numerical results obtained averaging 5 stochastic runs in Figures 4.10-4.11. From the last two plots of both figures, the effect of the seasonal variation of the preference coefficients can be clearly appreciated, and we observe that the epidemic tends toward an endemic state. The final distribution of the state variable v_2 also appears much more varied in both the configurations. On the other hand, the socio-physical variables seem to be less affected by the variability of α and β . To highlight this effect, in Figure 4.12 we show the bivariate distribution of the socio-physical condition of the whole population and of the viral impact related to infected agents at the final time of the simulations. Concerning only Test 3(b), in Figure 4.11 we can see that the death process appears significant only in the early stages of infectious disease spread and, instead, remains under control in the later stage of endemic equilibrium.

5 Conclusion

In this paper, we explore the realm of irreversibility in biological processes through the lens of utility theory, with a primary focus on viral evolution. This approach, drawing inspiration from microeconomics and the renowned Edgeworth box, complements existing models, such as those employing game theory to characterize viral behavior [10, 11]. Our utility-based modeling, formalized as a kinetic model of Boltzmann-type where a large number of agents interact through binary encounters, provides insights into the irreversibility of infectious diseases, particularly within the oscillatory nature observed in successive pandemic waves. The numerical experiments presented shed light on the mechanism steering these phenomena toward endemicity. In conclusion, this exploration, albeit preliminary, aims to lay the foundations for a new modelling approach to epidemiology and serves as a basis for further investigations into the complexity of infectious disease dynamics.

Acknowledgments

This work has been written within the activities of GNCS and GNFM groups of INdAM (Italian National Institute of High Mathematics). The research has been supported by the Royal Society under the Wolfson Fellowship “Uncertainty quantification, data-driven simulations and learning of multiscale complex systems governed by PDEs”. The partial support by ICSC – Centro Nazionale di Ricerca in High Performance Computing, Big Data and Quantum Computing, funded by European Union – NextGenerationEU and by MUR-PRIN Project 2022, No. 2022KKJP4X “Advanced numerical methods for time dependent parametric partial differential equations with applications” is also acknowledged. GB has also been partially funded by the call “Bando Giovani anno 2023 per progetti di ricerca finanziati con il contributo 5x1000 anno 2021” of the University of Ferrara, and by MUR PRIN 2022 PNRR Project No. P2022JC95T “Data-driven discovery and control of multi-scale interacting artificial agent systems”.

References

- [1] G. Albi, W. Boscheri, G. Bertaglia, G. Dimarco, L. Pareschi, G. Toscani, M. Zanella. Kinetic modelling of epidemic dynamics: social contacts, control with uncertain data, and multiscale spatial dynamics. In: *Predicting Pandemics in a Globally Connected World*, Vol. 1, N. Bellomo and M. Chaplain Eds., Springer-Nature (2022) 43–108.
- [2] V.V. Aristov. Biological systems as nonequilibrium structures described by kinetic methods. *Results Phys.* **13** (2019) 102232.
- [3] V.V. Aristov, A.S. Buchelnikov, Y.D. Nechipurenko. The use of the statistical entropy in some new approaches for the description of biosystems. *Entropy* **24** (2022) 172.
- [4] G. Bertaglia. Asymptotic-Preserving Neural Networks for Hyperbolic Systems with Diffusive Scaling. In: *Advances in Numerical Methods for Hyperbolic Balance Laws and Related Problems*, SEMA SIMAI Springer Series, G. Albi, W. Boscheri, and M. Zanella, Eds., Springer (2023) 23–48.
- [5] G. Bertaglia, W. Boscheri, G. Dimarco, L. Pareschi. Spatial spread of COVID-19 outbreak in Italy using multiscale kinetic transport equations with uncertainty. *Math. Biosci. Eng.* **18** (2021) 7028–7059.

- [6] G. Bertaglia, L. Liu, L. Pareschi X. Zhu. Bi-fidelity stochastic collocation methods for epidemic transport models with uncertainties. *Netw. Heterog. Media* **17** (2022) 401–425.
- [7] G. Bertaglia, C. Lu, L. Pareschi, X. Zhu. Asymptotic-Preserving Neural Networks for multiscale hyperbolic models of epidemic spread. *Math. Mod. Meth. App. Scie.* **32**(10) (2022) 1949–1985.
- [8] G. Bertaglia, L. Pareschi. Hyperbolic models for the spread of epidemics on networks: kinetic description and numerical methods, *ESAIM Math. Model. Numer. Anal.* **55** (2021) 381–407.
- [9] G. Bertaglia, L. Pareschi. Hyperbolic compartmental models for epidemic spread on networks with uncertain data: Application to the emergence of Covid-19 in Italy. *Math. Mod. Meth. App. Scie.* **31** (2021) 2495–2531.
- [10] K. Bohl, S. Hummert, S. Werner, D. Basanta, A. Deutsch, S. Schuster, G. Theisseng, A. Schroetera. Evolutionary game theory: molecules as players. *Mol. BioSyst.* **10** (2014) 3066–3074.
- [11] W. Casey, S.E. Massey, B. Mishra. How signalling games explain mimicry at many levels: from viral epidemiology to human sociology. *J. R. Soc. Interface* **18** (2021) 20200689.
- [12] C. Cercignani. *The Boltzmann equation and its applications*, Springer Series in Applied Mathematical Sciences, Vol. 67, Springer–Verlag (1988).
- [13] R. Della Marca, N. Loy, A. Tosin. An SIR–like kinetic model tracking individuals’ viral load, *Netw. Heterog. Media* **17**(3) (2022) 467.
- [14] Y. Demirel, Information in biological systems and the fluctuation theorem. *Entropy* **16** (2014) 1931–1948.
- [15] G. Dimarco, L. Pareschi, G. Toscani, M. Zanella. Wealth distribution under the spread of infectious diseases. *Phys. Rev. E* **102** (2020) 022303.
- [16] G. Dimarco, B. Perthame, G. Toscani, M. Zanella. Kinetic models for epidemic dynamics with social heterogeneity. *J. Math. Biol.* **83**(4) (2021).
- [17] F.Y. Edgeworth, *Mathematical Psychics: An Essay on the Application of Mathematics to the Moral Sciences*, Kegan Paul, London (1881).
- [18] M. Gatto, E. Bertuzzo, L. Mari, S. Miccoli, L. Carraro, R. Casagrandi, A. Rinaldo. Spread and dynamics of the COVID-19 epidemic in Italy: Effects of emergency containment measures. *PNAS*, **117** (19) (2020) 10484–10491.
- [19] G. Giordano, F. Blanchini, R. Bruno, P. Colaneri, A. Di Filippo, A. Di Matteo and M. Colaneri. Modelling the COVID-19 epidemic and implementation of population-wide interventions in Italy. *Nature Medicine* **26** (2020) 855–860.
- [20] N. Guglielmi, E. Iacomini, A. Viguerie. Delay differential equations for the spatially resolved simulation of epidemics with specific application to COVID-19. *Math. Mod. Meth. App. Scie.* **45**(8) (2022) 4752–4771.
- [21] W.O. Kermack and A.G. McKendrick. Contributions to the mathematical theory of epidemics, part 1, *Proc. Roy. Soc. London Ser. A*, **115** (1927), 700–721.

- [22] A.C. Lowen, S. Mubareka, J. Steel, P. Palese. Influenza virus transmission is dependent on relative humidity and temperature. *PLoS Pathog.* **3** (2007) 1470–1476.
- [23] N. Loy, A. Tosin. A viral load-based model for epidemic spread on spatial networks. *Math. Biosci. Eng.* **18**(5) (2021) 5635–5663.
- [24] C.J.E. Metcalf, O.N. Bjornstad, B.T. Grenfell, V. Andreasen. Seasonality and comparative dynamics of six childhood infections in pre-vaccination Copenhagen. *Proc. R. Soc. B. Biol. Sci.* **276** (2009) 4111–4118.
- [25] D.M. Morens, G.K. Folkers, A.S. Fauci. What is a pandemic? *The Journal of Infectious Diseases* **200** (2009) 1018–1021.
- [26] L. Pareschi, G. Russo. An introduction to Monte Carlo methods for the Boltzmann equation. *ESAIM: Proceedings* **10** (2001) 35–75 .
- [27] L. Pareschi and G. Toscani. *Interacting Multiagent Systems, Kinetic Equations And Monte Carlo Methods*. Oxford University Press (2013).
- [28] L. Pareschi and G. Toscani. Self-similarity and power-like tails in nonconservative kinetic models. *J. Stat. Phys.* **124**(2-4) (2006) 747–779.
- [29] G. Toscani, C. Brugna, S. Demichelis. Kinetic models for the trading of goods, *J. Stat. Phys.* **151** (2013) 549–566.
- [30] R. Zivieri, N. Pacini, G. Finocchio, M. Carpentieri. Rate of entropy model for irreversible processes in living systems. *Sci. Rep.* **7** (2017) 9134.